Use of Maximum Intensity Projections in CT Angiography: A Basic Review[1]

Mathias Prokop, MD
Hoen Oh Shin, MD
Ansgar Schanz, MD
Cornelia M. Schaefer-Prokop, MD

CME FEATURE

This article meets the criteria for 1.0 credit hour in Category 1 of the AMA Physician's Recognition Award. To obtain credit, see the questionnaire on pp 473–478.

LEARNING OBJECTIVES

After reading this article and taking the test, the reader will be able to:

- Understand the principles of MIP and its use in CT angiography.
- Optimize the scan parameters to achieve the best image quality in MIP CT angiograms.
- Understand the pitfalls of MIP CT angiography and ways to detect them.

Maximum intensity projection (MIP) is a simple three-dimensional visualization tool that can be used to display computed tomographic angiography data sets. MIP images are not threshold dependent and preserve attenuation information. Thus, they often yield acceptable results even in cases in which shaded surface display images fail because of threshold problems. MIP is particularly useful for depicting small vessels. Because MIP does not allow for differentiation between foreground and background, MIP images are best suited for displaying relatively simple anatomic situations in which superimposition of structures does not occur (eg, the abdominal aorta). If anatomic structures are superimposed over the vessel of interest, the MIP technique can provide images of diagnostic quality as long as the contrast of the vessel of interest is sufficiently high compared with that of surrounding structures. Editing procedures for MIP are usually used to exclude unwanted structures from the volume of interest and include cutting functions and region-growing algorithms. Artifacts from vessel pulsation and respiratory motion may occur and simulate abnormalities, but, with careful attention, they can be distinguished from real disease. MIP images should always be interpreted together with the original transaxial data set. Knowledge of display properties and artifacts is necessary for correct interpretation of MIP images and helps one create images of optimal quality, choose appropriate examination parameters, and distinguish artifacts from disease.

Abbreviations: MIP = maximum intensity projection, SSD = shaded surface display, VOI = volume of interest, 2D = two dimensional, 3D = three dimensional

Index terms: Computed tomography (CT), angiography, **.12916[2] • Computed tomography (CT), image processing Computed tomography (CT), maximum intensity projection, **.12916[2]

RadioGraphics 1997; 17:433–451

[1] From the Department of Diagnostic Radiology I, Hannover Medical School, Konstanty Gutschow Str 8, D-30623 Hanover, Germany. Recipient of a Magna Cum Laude award for a scientific exhibit at the 1995 RSNA scientific assembly. Received April 29, 1996; revision requested June 12; final revision received January 17, 1997; accepted January 17. **Address reprint requests to** M.P.

[2] ** indicates use of the technique anywhere in the body.

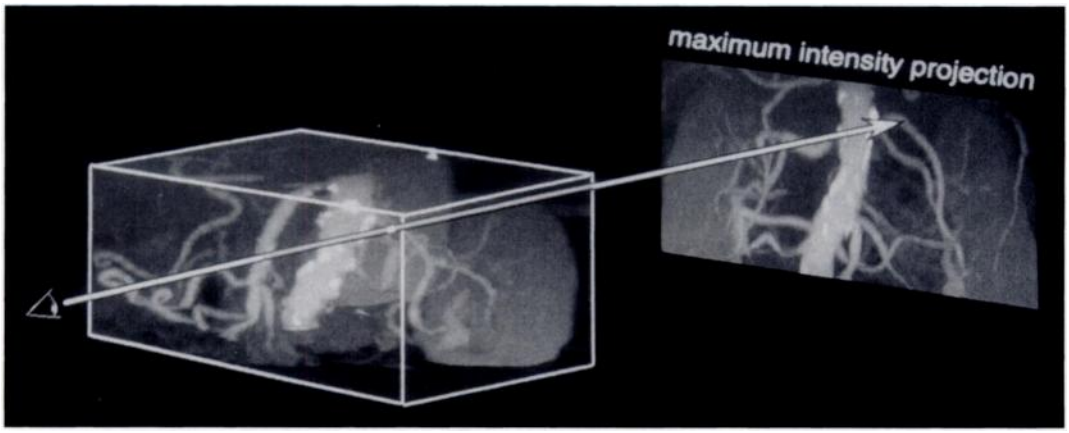

a.

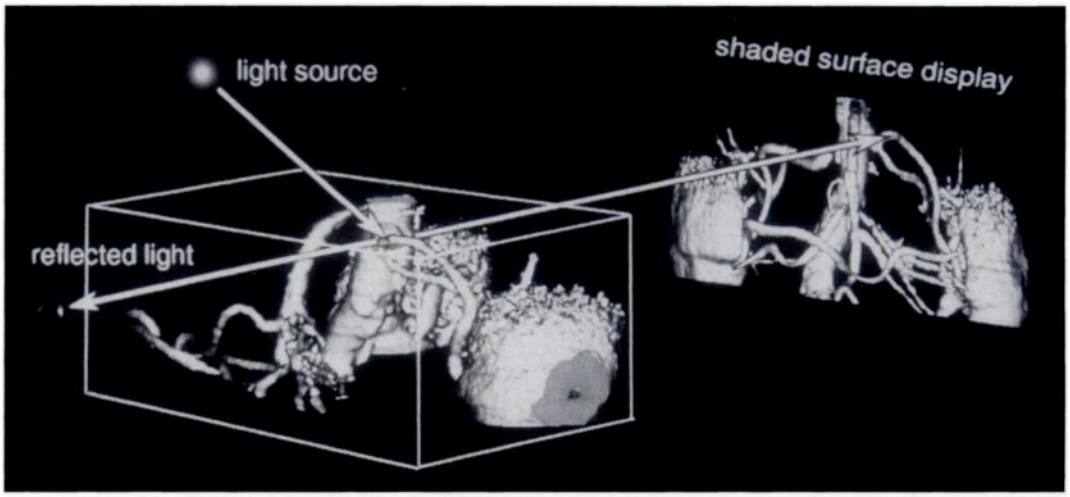

b.

Figure 1. **(a)** Diagram illustrates the basic principle of MIP: Parallel rays are cast through a VOI, and the maximum CT number along each projecting ray is displayed as an MIP image. **(b)** Diagram illustrates the basic principle of SSD: Rays are cast from a light source onto the surface of an object and are reflected or scattered according to surface orientation. The amount of light that reaches the eye of an observer determines the local gray value of each pixel in the view plane.

■ INTRODUCTION

Computed tomographic (CT) angiography is a minimally invasive technique for vascular imaging that is based on spiral or helical CT (1–5). To obtain an "angiographic" display of vascular structures, various three-dimensional (3D) rendering techniques are used to project the acquired data volume into a view plane. The most well known of these techniques are shaded surface display (SSD) and maximum intensity projection (MIP) (4). Newer volume-rendering techniques may combine the advantages of both methods, yielding a variety of effects such as semitransparent views, improved surface definition, and high-quality images in virtual endoscopic displays (6,7).

In this article, we review the basic principles of MIP as applied to CT angiography and discuss the display properties of this technique and the influence of various examination parameters on image quality. In addition, we describe various editing procedures for data preparation, as well as pitfalls for image interpretation and ways to detect them. Optimized strategies to obtain good results for various clinical imaging tasks are outlined.

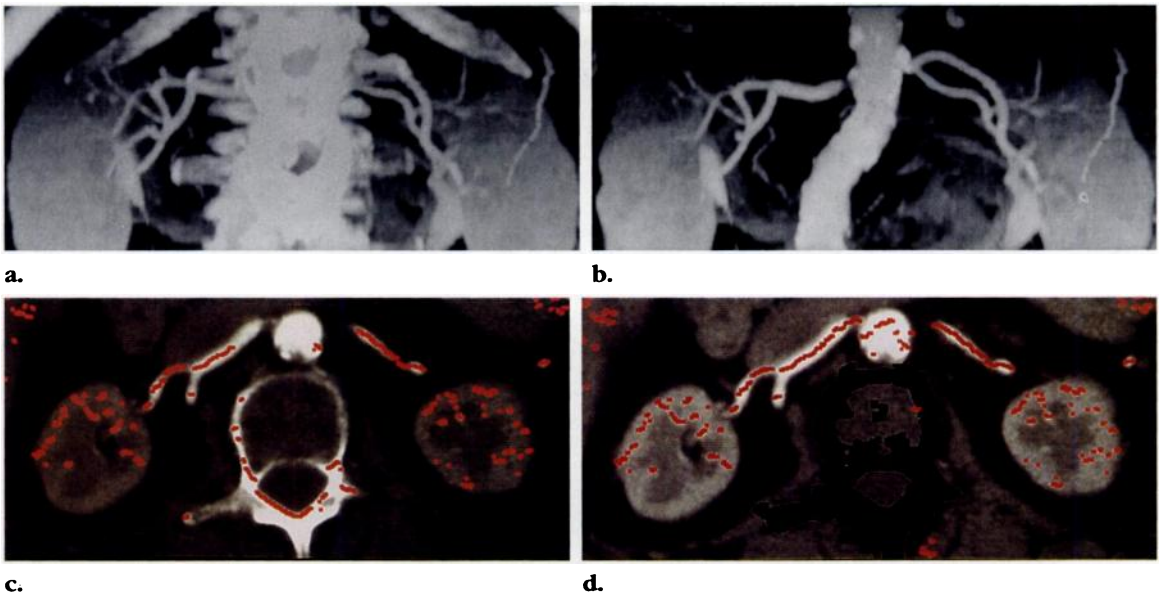

Figure 2. **(a, b)** Anteroposterior MIP images are shown before **(a)** and after **(b)** data editing to remove the skeletal structures. **(c, d)** Corresponding transaxial images before **(c)** and after **(d)** data editing are displayed in which the projected voxels (those with maximum CT number in the anteroposterior viewing direction) are highlighted in red.

■ PRINCIPLES OF MIP

MIP is a simple volume-rendering technique. For a given viewing direction, parallel rays are cast through a volume of interest (VOI), and the maximum CT number encountered along each ray is displayed (Fig 1a). This VOI is determined from a stack of transaxial spiral CT images. For CT angiography, various editing procedures are used to exclude structures that might be superimposed over the vessel of interest. Bones usually have a higher CT number than contrast material–enhanced vessels and will be preferentially displayed on MIP images (Fig 2a). Thus, exclusion of bones is necessary for most applications of CT angiography (Fig 2b).

Data editing can be avoided if only a few transaxial images are used to produce MIP images (a technique known as thin-slab MIP) in a caudocranial viewing direction. For interactive viewing, this slab can then be moved through the whole stack of transaxial images (ie, sliding thin-slab MIP images) (8).

In contrast to MIP, SSD requires the definition of a 3D binary object. This object is then illuminated by a virtual light source, and the resulting reflections from the object surface determine the local gray values on the SSD image (Fig 1b).

SSD images contain depth information about the object surface (foreground and background discrimination), but most SSD variants do not retain attenuation information from inside an object. In contrast, MIP images do not provide depth information, but they do contain attenuation information (eg, about vascular calcifications). Although SSD requires precise definition of the vessel of interest, MIP needs to exclude only disturbing overlying structures from the VOI to produce diagnostically useful images.

• Projection Effects

Differentiation between foreground and background is not possible on a single MIP image. On an MIP image, the voxel with the highest CT number is displayed, independent of the voxel position along the projecting ray (Fig 3). As a consequence, various projection effects occur. To achieve a 3D effect, one must view multiple MIP images from slightly varying viewing angles (cine display).

Whenever the projecting ray hits a contrast-enhanced voxel, that voxel is displayed preferentially over voxels of soft-tissue attenuation

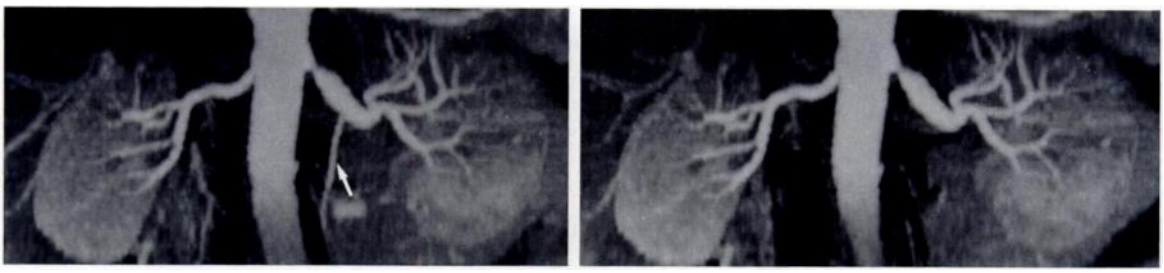

a. b.

Figure 3. **(a)** On an anteroposterior view of the renal arteries, the presence of a large ovarian artery (arrow) was suspected. **(b)** With a narrower VOI, a superprojecting side branch of the superior mesenteric artery could be excluded, and the resulting MIP image demonstrates the normal anatomy (with a stenosis of the left renal artery). MIP images do not provide depth information.

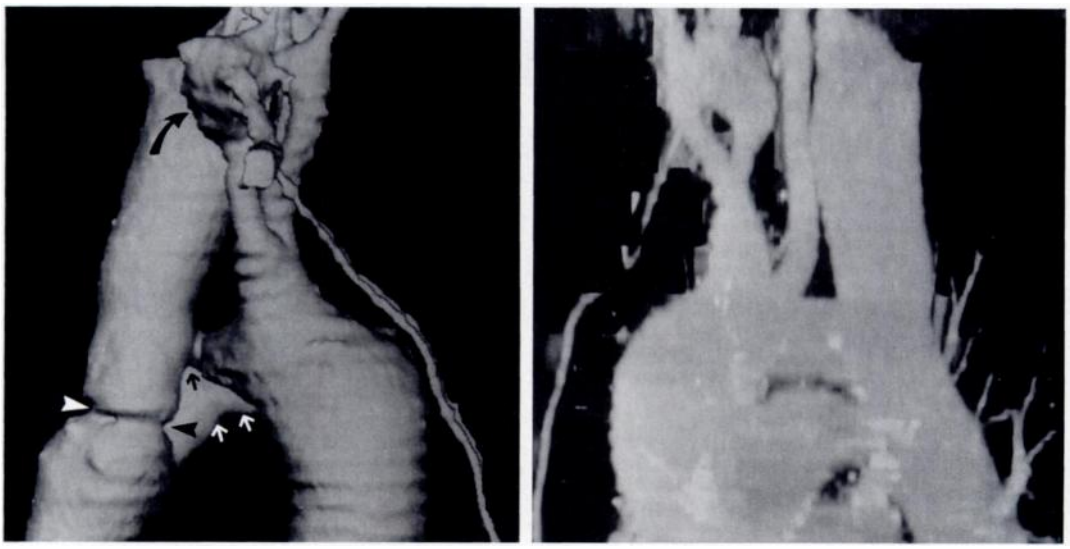

a. b.

Figure 4. SSD **(a)** and MIP **(b)** images demonstrate a complex anomaly of the aorta. The SSD image clearly depicts a hypoplastic aortic arch (straight black arrow), a persistent coarctation (arrowheads), bilateral subclavian aneurysms (of which only one is seen en face, curved arrow), and an extra-anatomic aortic bypass graft (white arrows). Independent of the viewing angle, a sufficient display of the abnormality was not possible with MIP.

values. Thus, concave regions may be superimposed by surrounding voxels, depending on the viewing direction. This "silhouette effect" produces a shadowlike image (Fig 4b). Because of this projection effect, MIP images are well suited for display of simple vascular anatomy (eg, the abdominal aorta) but are not useful for visualization of complex anatomic situations with superprojecting vessels (Fig 4) (2,8).

MIP images do not allow visualization of hypoattenuating intraluminal abnormalities. Intraluminal thrombi (Fig 5) or pulmonary emboli can be detected only if they are directly adjacent to the vessel wall or if the CT numbers of the remaining contrasted vessel lumen are reduced because of partial volume averaging. In MIP images of an aortic dissection in which the true and false channels are enhanced to the same degree, dissecting membranes must lie parallel to the viewing direction to be directly visualized (Fig 6) (9). Curved membranes cannot be seen. If there is a perfusion difference, however, MIP is sensitive in the depiction of the aortic dissection, but the width of the channel with the higher CT numbers (usually the true channel) will usually be overestimated.

In general, MIP images are better suited for depicting the abdomen and pelvis than the chest. There are disease entities and anatomic situations in which the MIP technique may fail in individual cases.

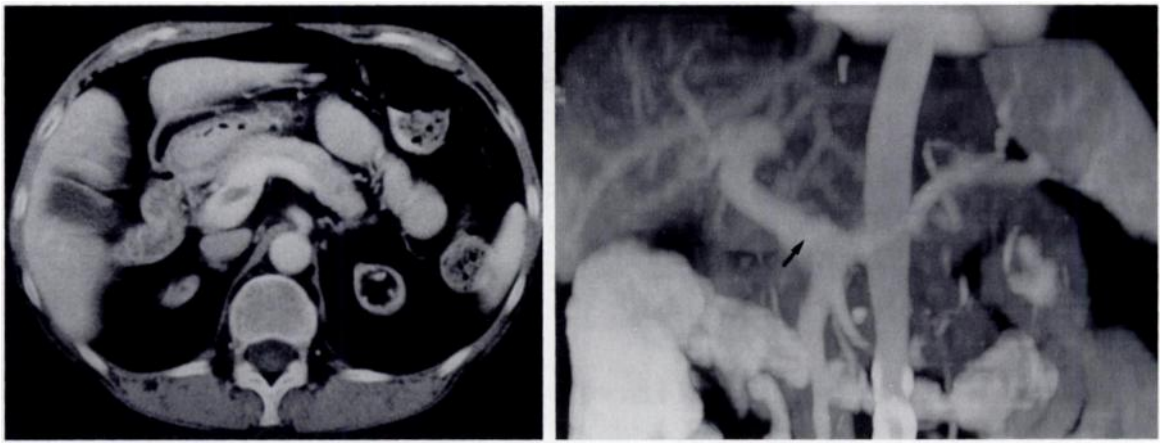

a. b.

Figure 5. **(a)** Axial CT scan shows a floating thrombus in the portal vein. **(b)** On the anteroposterior MIP image, this finding is completely missed. Arrow indicates where the thrombus should have been found.

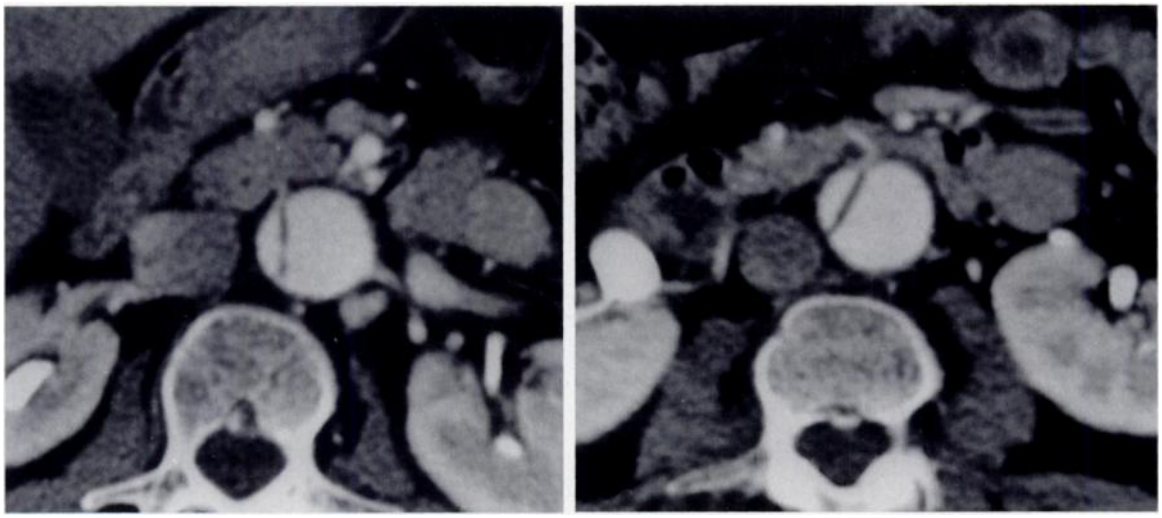

b. c.

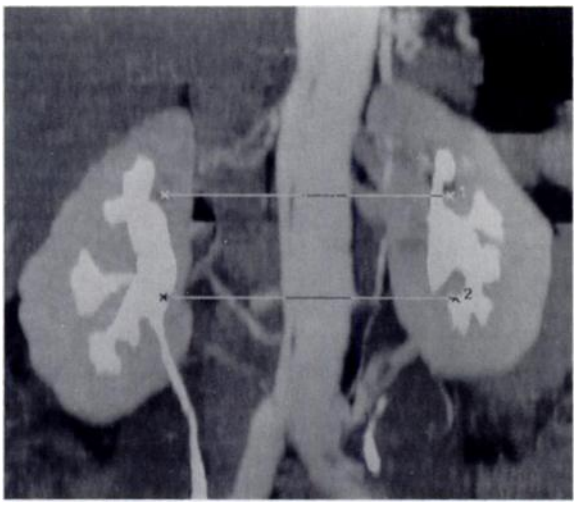

a.

Figure 6. Anteroposterior MIP image **(a)** and axial CT scans **(b, c)** obtained at levels *1* and *2* show a chronic aortic dissection with identical enhancement of both channels. The MIP image demonstrates only those portions of the membrane that run exactly parallel to the viewing direction.

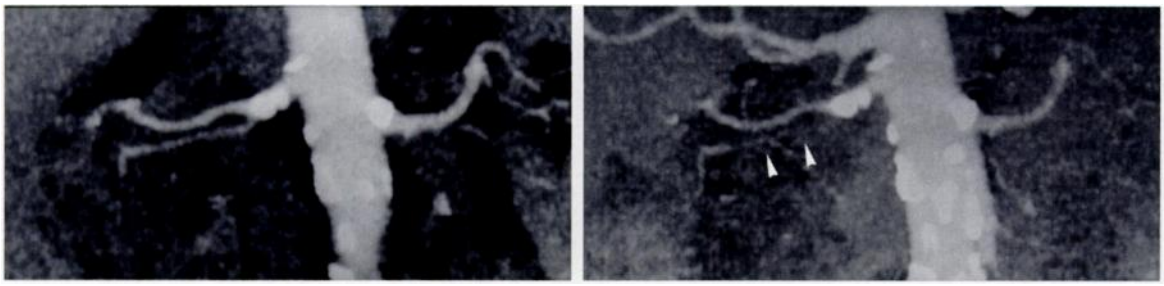

a. b.

Figure 8. Anteroposterior MIP images reconstructed with a narrow VOI **(a)** and a wide one **(b)** demonstrate the renal arteries. The vessels have identical brightness on both MIP images, but the background attenuation is increased with use of the wide VOI **(b)**. As a result, the lower branch of the right renal artery is completely masked by background attenuation (arrowheads). The calcified plaques at the renal artery orifices completely obscure the arterial lumen independent of the VOI.

• VOI Width

In MIP images, the attenuation of vascular structures (maximum CT number) is not affected by the size of the VOI. The attenuation of the soft-tissue background, however, grows with increasing width of the VOI because the chance of encountering larger CT numbers increases with the length of the ray path within the VOI. There are two main reasons for this: statistical variations among CT numbers due to image noise and inclusion of organs with higher CT numbers.

Image noise is particularly high in adipose patients and is increased by use of low milliampere seconds or standard (instead of smoothing) reconstruction algorithms. The probability of encountering larger CT numbers grows with higher noise levels and with increasing path length through the (noisy) soft-tissue background. Thus, the attenuation of a homogeneous tissue sample on an MIP image is determined by the average CT number of this tissue, the image noise, and the width of the VOI (path length). With growing path lengths, there is at first a rapid increase in background attenuation. At VOI widths greater than a few centimeters, the change in background attenuation becomes very small (Fig 7).

Background attenuation also increases as organs enhance with contrast material. During the course of spiral CT data acquisition (usually 20–40 seconds), organ enhancement increases; thus, the background attenuation will also increase toward the end of the scan. Organ enhancement is strongest in the abdomen (kidney, spleen, liver, and bowel) and in the neck (thyroid). The greater the number of enhancing structures included in the VOI, the larger the probability that the background attenuation will exceed the CT number of a vessel of interest (Fig 7). The vessel will then be lost on the MIP image (Fig 8).

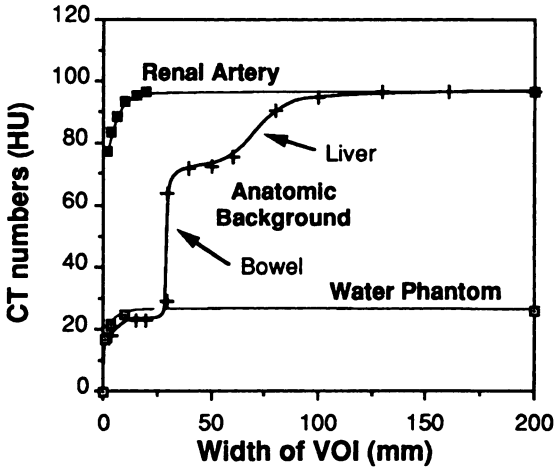

Figure 7. Graph demonstrates the effects of background CT numbers on an MIP, displayed as a function of VOI width. The background attenuation consists of image noise (from a homogeneous 20-cm water phantom) and inclusion of enhancing overlying organs (same case as in Fig 8, with use of a paracaval VOI). For comparison, the attenuation of a small renal artery (right-sided lower branch on Fig 8) is displayed.

Background attenuation increases most strongly if overlying vessels are included in the VOI. The effect of overlying vessels is strongest in the chest. With MIP, there is no separation of pulmonary arteries and veins, and pulmonary vessels are superimposed over the aorta (Fig 4). In the abdomen, there is superprojection of renal and portal veins (Fig 9). In the neck, the jugular veins may obscure the carotid arteries. If possible, overlying vessels should be excluded by using editing procedures. In many cases, removal of an overlying vessel is the only way that the vessel of interest can be evaluated sufficiently.

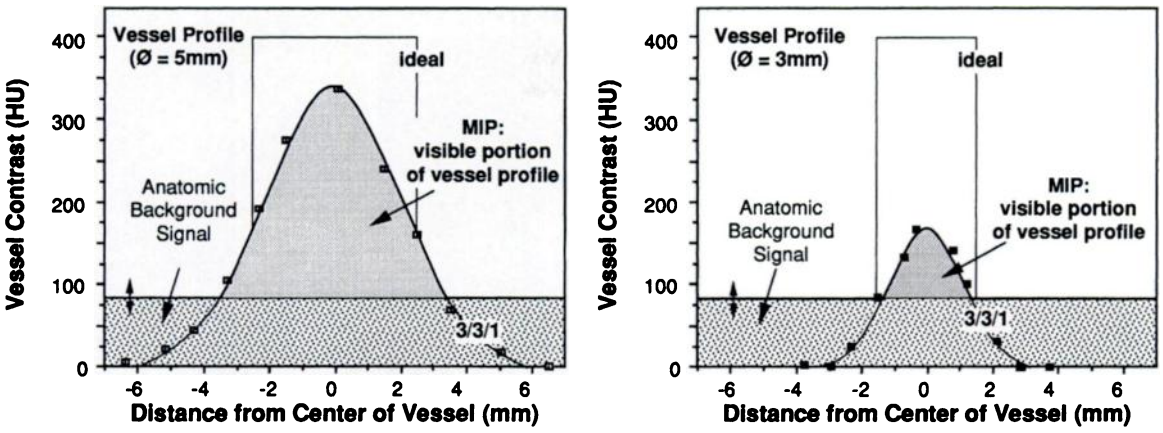

Figure 10. Graphs illustrate the effect of background attenuation on vessel diameter. Vessel profiles along the z axis were measured for simulated vessels of 5-mm **(a)** and 3-mm **(b)** diameter that ran parallel to the scan plane. The ideal rectangular profiles are also provided. The apparent vessel diameter can be derived from the attenuation profile of a vessel and the level of the background attenuation. With increasing background attenuation, edge pixels are no longer displayed and the apparent vessel size decreases.

a.

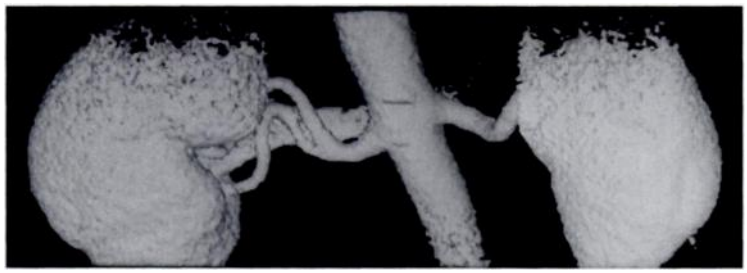

b.

Figure 9. **(a)** Anteroposterior MIP image of the renal arteries demonstrates enhancement of an overlying renal vein (arrow). This locally increased background attenuation decreases the apparent size of the left renal artery, suggestive of a moderate stenosis. **(b)** Posterior SSD image demonstrates the normal vessel size.

As background attenuation increases, apparent vessel size in MIP images decreases. This is due to partial volume averaging. Vessels that run parallel to the scan plane are blurred along the patient axis (z axis). Depending on the background attenuation, a varying amount of voxels at the border of the vessel will lie below this attenuation value and thus will not be displayed. The higher the background attenuation, the smaller the displayed cross section of the vessel.

This effect can be quantified when the attenuation profile ("vessel profile") of such a vessel is determined by measuring the CT numbers along a cross-sectional line parallel to the z axis through the center of the vessel. Ideally, the vessel profile should be rectangular (CT numbers higher than those of the background are measured only in the vessel and not outside). In reality, the vessel profile has a rounded shape (Fig 10). Only those portions of the vessel profile with CT numbers larger than the background attenuation will contribute to the resulting MIP image. With increasing background attenuation, the vessel "drowns" in the

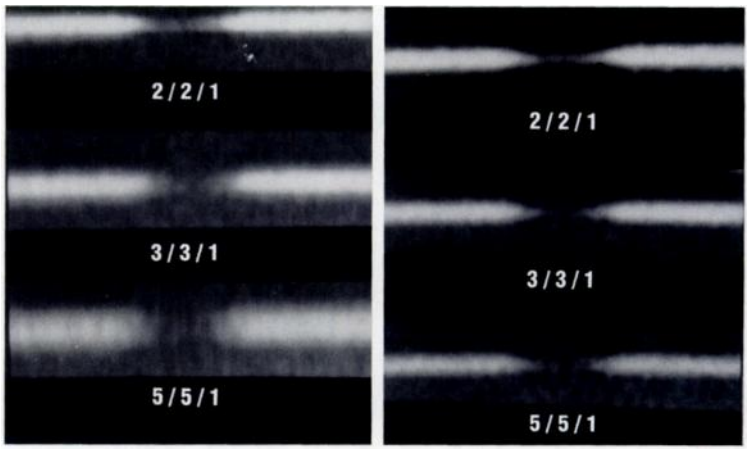

a. b.

Figure 11. Images of a phantom illustrate influence of scan parameters on z-axis distortion and apparent vessel contrast. Anteroposterior **(a)** and caudocranial **(b)** views show a vessel phantom with a simulated stenosis that was parallel to the scan plane. Parameters are given as a triplet of numbers: collimation/table feed/reconstruction increment (values in millimeters). Although there is marked distortion along the z axis in the anteroposterior views with increasing collimation, only a reduction in contrast is visible on the caudocranial views. Note that a pseudo- occlusion develops on these latter images with larger collimation.

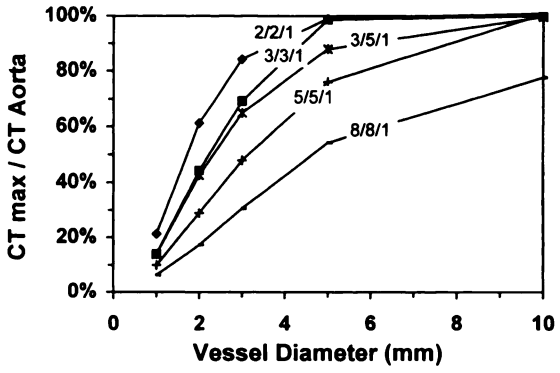

Figure 12. Graph depicts maximum CT numbers measured in a vessel phantom (horizontal vessel course) and expressed as a percentage of the theoretic value. Scan parameters are given as a triplet of numbers: collimation/table feed/reconstruction increment (all values are in millimeter). Note that vascular contrast decreases rapidly if vessel diameter falls below 3 mm. The effect is less pronounced for larger pitch factors (eg, comparing 3/5/1 and 5/5/1). The vascular contrast diminishes with increasing effective section thickness.

background, and the apparent vessel size decreases (Fig 10). The effect is most pronounced for small vessels (Fig 10b) and may even simulate vessel occlusion (Fig 8).

As a result, the width of the VOI must be chosen to be as narrow as possible to reduce background attenuation and to increase the conspicuity of vascular structures. All disturbing overlying structures should be excluded. The advantages of a narrow VOI and interactive viewing are combined when sliding thin-slab MIP images are used (8).

• Object Distortion and Scan Parameters

Increasing the effective section thickness leads to increased image distortion along the z axis. Vessels that run parallel to the scan plane (eg, renal arteries, circle of Willis) are most strongly affected by partial volume averaging: The vessel profile widens along the z axis, and the vessel contrast decreases (Figs 11, 12) (10–12).

The choice of scan parameters is determined by the required scan range and the possible scan time (usually the time that the patient is able to hold his or her breath). From this, the necessary table feed per rotation is determined. To cover the scan range with the smallest possible effective section thickness, the collimation should be reduced as much as possible. This is equivalent to increasing the pitch factor (table feed ÷ collimation). The pitch factor, in general, should not be increased above a value of 2.0, since this causes undersampling of data and may lead to artifacts (13). For optimal results, use of a 180° interpolation algorithm is required (Table) (14). Figure 13 demonstrates that the vessel profile along the z axis improves (for a constant table feed, such as 5 mm per rotation) if the collimation is reduced (eg, from 5 mm to 3 mm, thus increasing the pitch from 1.0 to 1.6).

Influence of Scan Parameters on Effective Section Thickness (at an Identical Volume Coverage per Time)

Scan Parameters			Effective Section Thickness (mm)*	
Collimation (mm)	Table Feed per Rotation (mm)	Pitch	360° Interpolation	180° Interpolation
6	6	1.0	10.0	7.1
5	6	1.2	9.5	6.4
4	6	1.5	9.0	5.7
3	6	2.0	8.5	5.0

* The effective section thickness is given as full-width-at-tenth area, calculated according to reference 13.

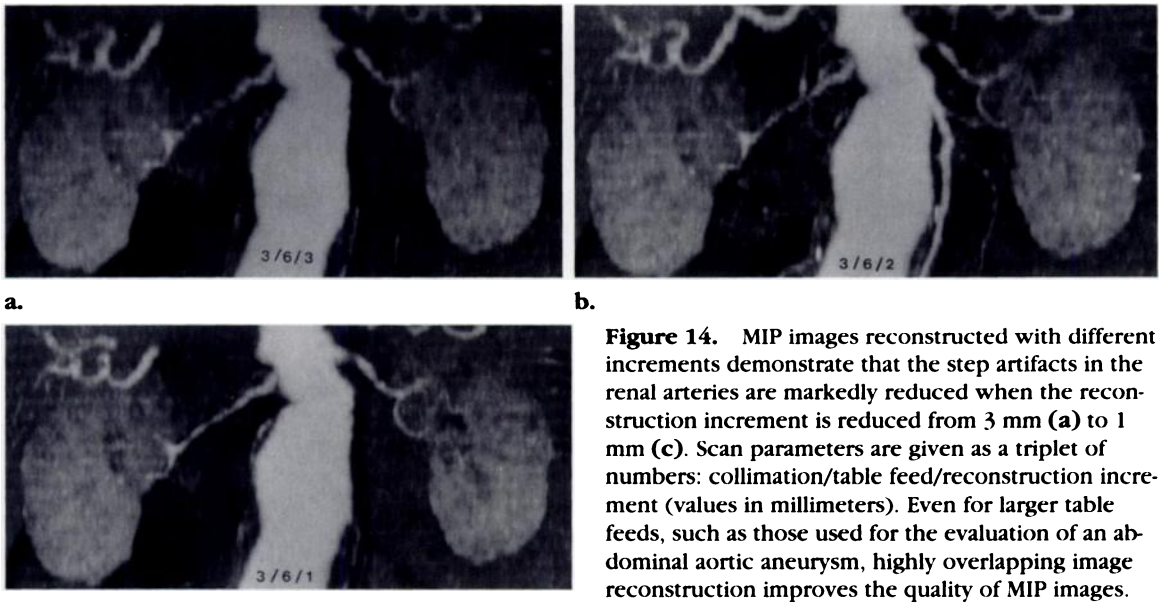

a. b. c.

Figure 14. MIP images reconstructed with different increments demonstrate that the step artifacts in the renal arteries are markedly reduced when the reconstruction increment is reduced from 3 mm **(a)** to 1 mm **(c)**. Scan parameters are given as a triplet of numbers: collimation/table feed/reconstruction increment (values in millimeters). Even for larger table feeds, such as those used for the evaluation of an abdominal aortic aneurysm, highly overlapping image reconstruction improves the quality of MIP images.

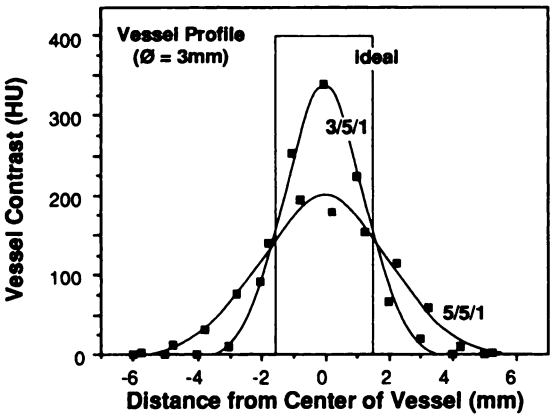

Figure 13. Graph shows the effects of changing pitch. With a table feed of 5 mm, a reduction of collimation from 5 mm (pitch = 1.0) to 3 mm (pitch = 1.6) leads to a narrower vessel profile and less contrast reduction due to partial volume averaging effects. For optimal z-axis resolution at a given scan range, pitch factors greater than or equal to 1.5 should be used.

A smoothing reconstruction algorithm should be used to reduce image noise and thus background attenuation. Because the CT numbers of vessels are hardly affected, the result is an increase in contrast of vascular structures on MIP images.

If vessels of interest in the MIP images have a horizontal course (ie, parallel to the scan plane), the reconstruction interval should be as small as reasonably possible (1–2 mm) to avoid generating step artifacts, since these artifacts may resemble stenoses (Fig 14). With narrow collimation (0.5–2 mm), the reconstruction interval should be less than or equal to half the table feed per rotation (ie, 0.2–1.0 mm).

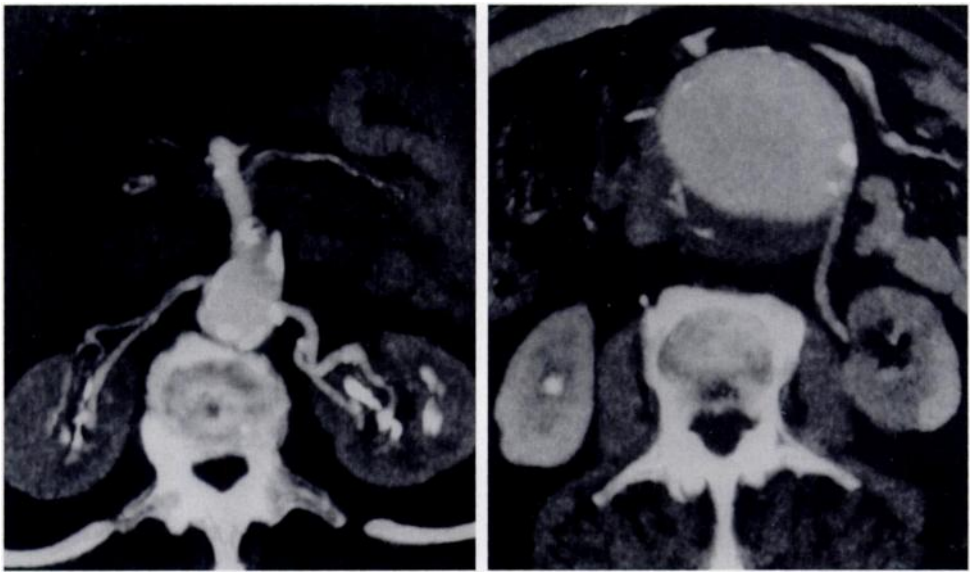

b. c.

a.

Figure 15. Anteroposterior MIP **(a)** and caudocranial thin-slab MIP **(b, c)** images show an abdominal aortic aneurysm with multiple renal arteries (arrows in **a**). The spatial resolution in the caudocranial projection is higher, and on **c**, an accessory left renal artery that originates from the aneurysm is detected. On the anteroposterior image **(a)**, this vessel was superimposed by the lumen of the aneurysm. Note that the proximal portion of the aneurysm is relatively low in attenuation; this appearance is due to turbulent slow flow in the aneurysm. Unenhanced blood is slowly exchanged by contrast-enhanced blood and will remain hypoattenuating during the earlier phases of the scan.

Frontal and lateral views are most affected by distortion artifacts (along the z axis), whereas axial views in craniocaudal or caudocranial direction are not influenced (Fig 15). However, partial volume averaging leads to reduction in contrast of small vessels even on axial views if larger collimations are used (Fig 11).

In conclusion, one should select the smallest possible effective section thickness at a given table feed (in general, pitch ≥ 1.5), use smoothing image reconstruction, and try a craniocaudal view in problematic cases. However, eccentrically located abnormalities may be visible only in two orthogonal planes.

• Vascular Contrast

The vascular contrast against the background attenuation determines the vessel size in the MIP image. For a given anatomic area, the background attenuation does not grow much with increasing vascular enhancement, as long as parenchymal organs and overlying vessels are excluded from the VOI. Under these conditions, the diameter of a vessel depends solely on the vascular contrast; that is, the difference in attenuation between vessel and background (Fig 16).

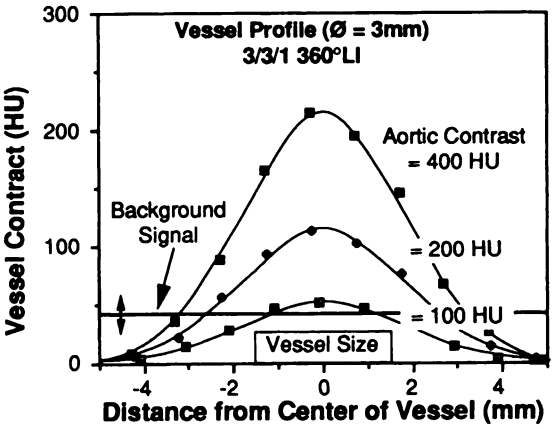

Figure 16. Graph illustrates that the height of the attenuation profile of an artery depends on the maximum aortic contrast. For a given background attenuation, the apparent vessel diameter decreases with lower vascular contrast.

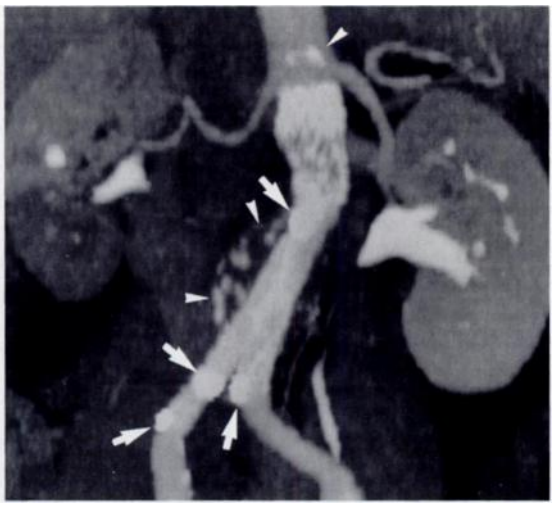

Figure 17. MIP image demonstrates an abdominal aortic aneurysm after treatment with an aortic stent prosthesis. The mural calcification outlines the thrombosed portion of the aneurysm. Note the difference in CT numbers of the aortic lumen, calcifications (arrowheads), nitinol stent, and platinum markers (arrows). Thrombus and wall calcifications can be directly visualized in large aneurysms if a narrow VOI (anteroposterior width less than the diameter of the aneurysm) is used. In this case, an accessory renal artery on the right side had been sacrificed. The resulting hypoperfusion of the lower pole of the kidney is seen.

Vessel contrast depends on the parameters used for injecting the contrast material; vascular enhancement increases with flow rate and concentration of the contrast medium. However, vascular enhancement depends even more greatly on cardiac output and the resulting dilution effects: A high output (such as occurs in young or anxious patients) reduces vascular enhancement, whereas a low cardiac output (such as occurs in older patients or those with left-sided heart failure) increases the enhancement.

Vessel contrast on MIP images also depends on partial volume averaging effects. Partial volume averaging most strongly affects small vessels that run parallel to the scan plane (Figs 11, 12). As a result, vessel contrast may be markedly reduced if the chosen effective section thickness considerably increases the vessel size.

In cases in which the vessel of interest will be subject to strong partial volume averaging (such as accessory renal arteries in MIP images of the abdominal aorta), one must attempt to achieve the highest possible vascular contrast. For MIP images of the neck, chest, pelvis, and extremities, vascular contrast is less critical.

• Calcifications

Calcifications and metal stents, clips, or markers have higher CT numbers than do vessels and therefore appear as bright spots on MIP images. Thus, MIP provides valuable information about the presence and distribution of vascular calcifications and the position of vascular stents (Fig 17) (3). However, small calcifications may not be seen if their CT number is in the range of the opacified vascular lumen, especially if large section thicknesses are used.

Vessel wall calcifications can obscure information about the vascular lumen if they are superimposed on the vessels (Fig 8). Changing the viewing direction (eg, using a caudocranial view) may help. In addition, partial volume

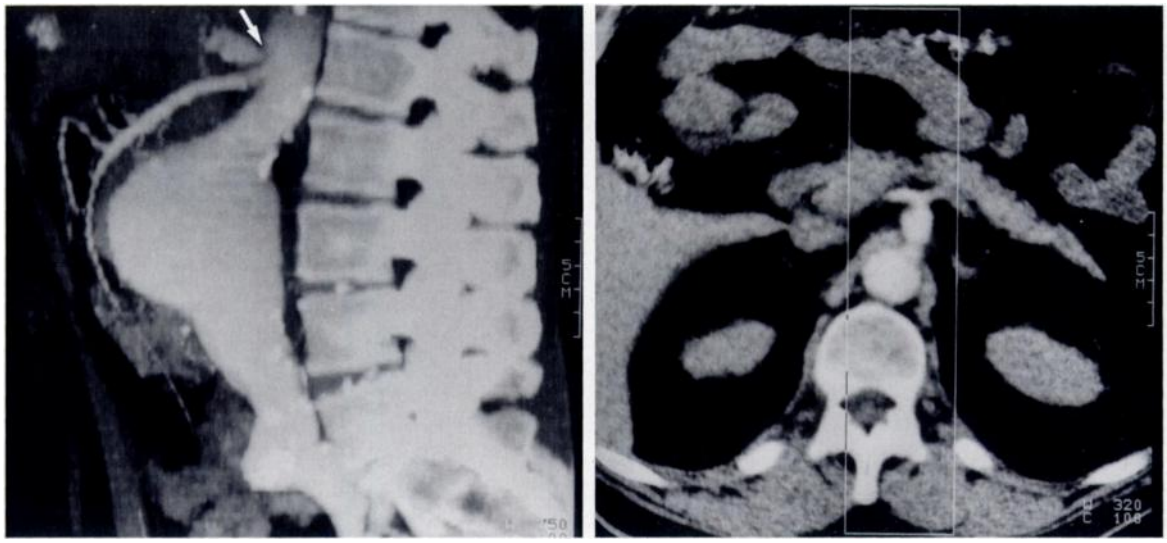

a. b.

Figure 19. **(a)** Lateral MIP image shows the proximal portion of the celiac artery and the superior mesenteric artery. Note the stenosis of the celiac artery (arrow) (the patient had an abdominal aortic aneurysm). **(b)** Corresponding axial section demonstrates how a narrow sagittal VOI can exclude the overlying parenchymal organs (kidneys, liver, spleen) without further editing.

averaging of calcification and vessel lumen may lead to overestimation of the size of calcified plaques. Frequently, the true width of the lumen cannot be reliably evaluated.

In conclusion, calcifications are easy to detect on MIP images, but they may compromise evaluation of the arterial lumen.

■ DATA EDITING

Various editing procedures are available to remove bones or other disturbing structures from the VOI. This process is called image segmentation. Editing procedures for MIP are usually used to exclude unwanted structures from the VOI ("negative editing") and typically are less time-consuming than actively including only vessels of interest in the VOI ("positive editing"), as is done for SSD (15). Image segmentation may be complex and time-consuming. Therefore, it is important to know how to use editing procedures effectively and when editing can be avoided altogether.

• Simplifications

In some situations, it is not necessary to perform true data editing to obtain MIP images of diagnostic quality; other simpler adjustments may be sufficient. For example, in abdominal MIP images (eg, of the renal artery orifices or celiac vessels), a caudocranial projection that is slightly tilted depending on the curvature of the spinal column may be diagnostic (Fig 18) if the width of the VOI is small enough (thin-slab MIP). Use of a narrow, rectangular VOI may suffice for demonstrating the central pulmonary

Figure 18. Caudocranial MIP image that has been tilted 10° toward the z axis demonstrates occlusive disease of the celiac artery and superior mesenteric artery. No editing is required because skeletal structures do not disturb evaluation of the image.

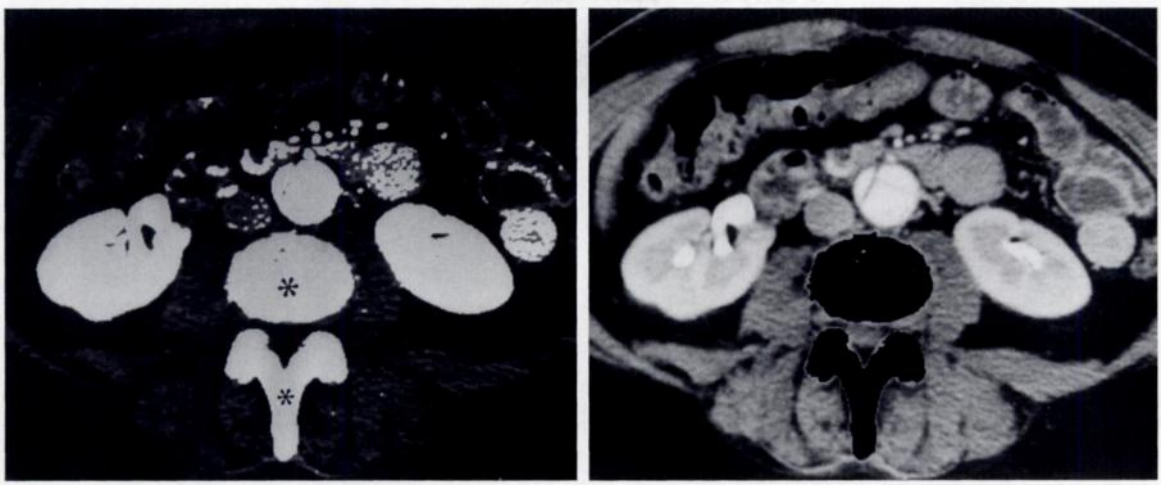

a. b.

c.

Figure 20. Images illustrate the results of using 2D region-growing algorithms to remove bone from the display. **(a, b)** On an axial image, a suitable threshold range is determined and seed points (*) are placed within the bones. All pixels that lie within the threshold range and are connected to the seed points are then detected and removed, as shown in **b**. **(c)** Axial image after bone removal with too high of a threshold retains bone contours (arrowheads) that will lead to ghost artifacts on MIP images.

vessels in an anteroposterior projection or the visceral arteries in a lateral projection (Fig 19).

• Basic Editing

There are two main editing procedures for removing bones or other unwanted structures from the MIP images: region-growing algorithms and cutting functions. The first step in using a region-growing algorithm is to choose an appropriate range of CT numbers (ie, the threshold range) to include the structures to be removed. To remove bones, one would use a range of 100–3,000 HU. Next, a "seed point" is placed in each bone structure (Fig 20a), and a region-growing algorithm is employed to tag and remove all voxels that are connected with the seed and that have CT numbers within the threshold range (Fig 20b). The threshold must be set low enough (just a little higher than the background, but well below the contrast of the smallest vessel) to ensure that faint bone contours are also removed and do not appear as ghost artifacts in the final MIP image (Fig 20c). For speed of handling, 3D region-growing algorithms are superior to 2D section-by-section region-growing algorithms. The 3D region-growing algorithms may be helpful for producing MIP images of the neck, abdomen, and pelvis.

For pure region-growing algorithms to work successfully, there must not be any connection between bone and vessel within the chosen threshold range. Otherwise, the seeding procedure will lead to an overflow into structures that were not intended to be tagged. In these cases, cutting or other separation functions must be employed locally to separate wanted from unwanted objects.

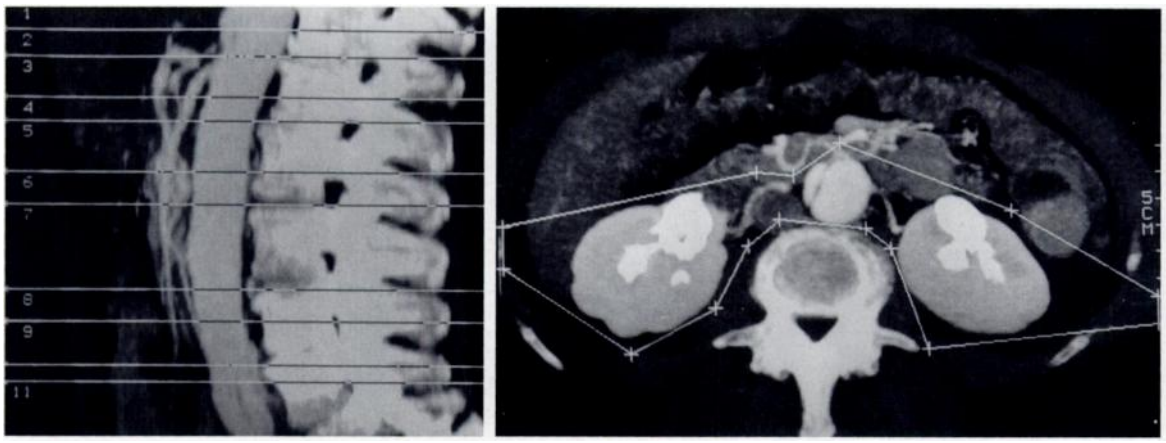

a. b.

Figure 21. **(a)** Lateral MIP image shows the subdivision of the data volume into multiple slabs, a procedure conducted with slab editors. **(b)** Caudocranial MIP image of each slab is then used to cut out unwanted structures simultaneously from all transaxial images in the slab.

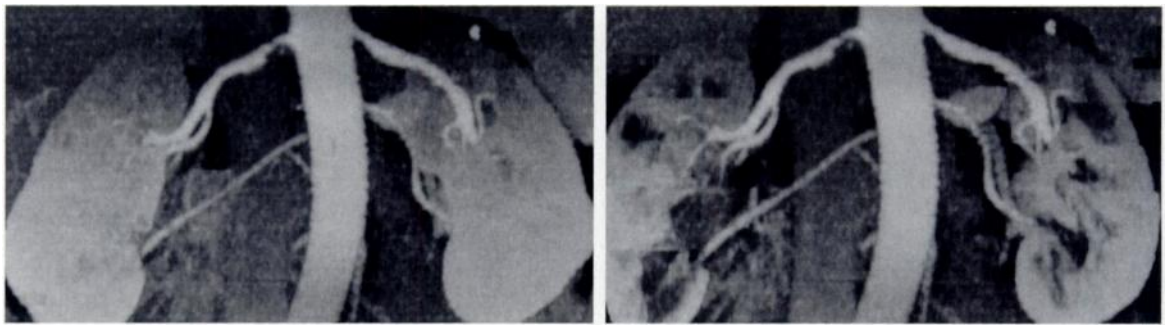

a. b.

Figure 22. **(a, b)** Anteroposterior MIP images formatted with standard algorithms **(a)** and with an algorithm to remove the renal parenchyma **(b)** demonstrate renal artery stenosis. **(c)** Representative transaxial image shows the corresponding VOI for the algorithm used in **b**. By removing most of the renal parenchyma, smaller renal artery branches at the renal hilum can be seen in **b**.

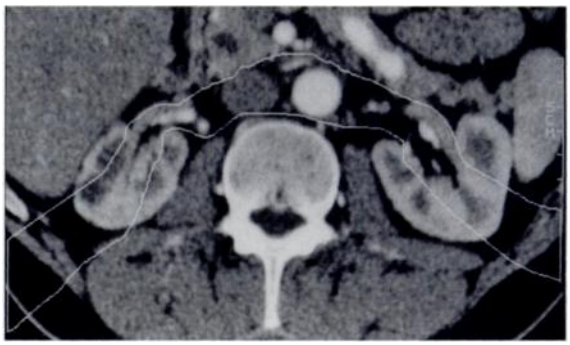

c.

Morphologic algorithms, such as erosion or dilation functions, can occasionally be used to separate bone from vessels of interest. In areas in which there is close contact between bones and vessels, the contact zone may be opened by removing the superficial voxel layer (erosion operators). The bones are then marked by using the seeding and region-growing algorithms and are subsequently processed by adding one voxel layer (dilation operators). In some cases (eg, images of the skull base, neck, or abdomen), this procedure yields reasonable results.

Cutting functions, which allow for interactively cutting away disturbing structures (usually bone), are generally easier to handle. Cutting can be done by placing appropriate regions of interest on each transaxial image and modifying these regions as one goes through the complete stack of transaxial images. More convenient techniques include the use of slab editors (Fig 21) or 3D editors that allow for simultaneous processing of a stack of images.

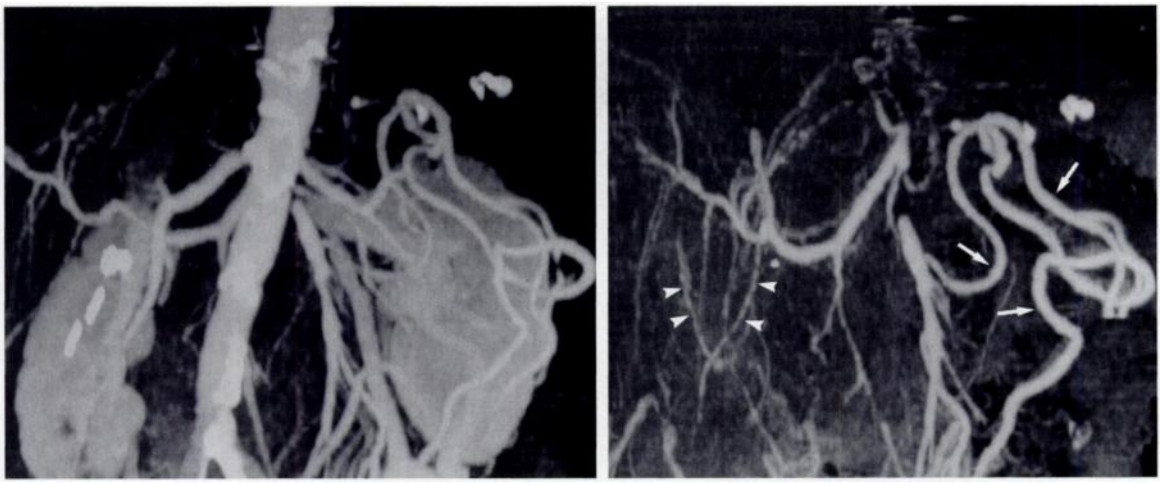

a. b.

Figure 23. Standard MIP **(a)** and selective MIP **(b)** images show occlusion of the celiac artery and superior mesenteric artery (same case as in Fig 18). The selective image, in which the aorta and kidneys have been removed, more clearly demonstrates the collateral pathway (arrows) and the capsular artery (arrowheads).

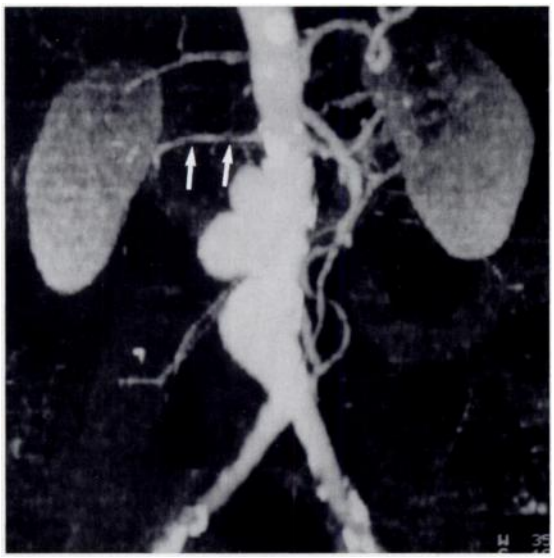

Figure 24. MIP image of a patient with an aortic aneurysm demonstrates a pulsation artifact that simulates renal artery stenosis (arrows).

• Advanced Editing

In some cases, it can be advantageous to remove structures other than bone to achieve a superior display of the vessel of interest. For example, in MIP images of the kidney, removal of overlying contrast-enhanced renal parenchyma leads to better visualization of intrarenal arterial branches (Fig 22). Similarly, removal of the aorta will yield an excellent overview of mesenteric or hepatic vessels in an anteroposterior projection (Fig 23). The resulting image is similar to that achieved by selective intraarterial angiography.

In summary, for selective imaging tasks, the complexity of the editing procedures can be markedly reduced. However, the more complex the imaging task is, the more complex the editing procedure must be. As the use of CT angiography becomes more widespread, semiautomated techniques for complex editing tasks will need to be developed.

■ CT ANGIOGRAPHY–RELATED ARTIFACTS AND PITFALLS

• Pulsation Artifacts

Vessel pulsation leads to undulating contours (eg, in the ascending aorta or aortic arch) or fine serration (eg, in the renal arteries), depending on table speed and pulse frequency. Pulsatile movements of renal arteries can simulate or obscure stenoses (Fig 24), although pulsation artifacts are in general easy to detect. Image reconstruction with a 360° interpolation algorithm rather than a 180° interpolation algorithm reduces the artifact (Fig 25) because data are averaged over a larger time interval (two rotations instead of slightly more than one rotation).

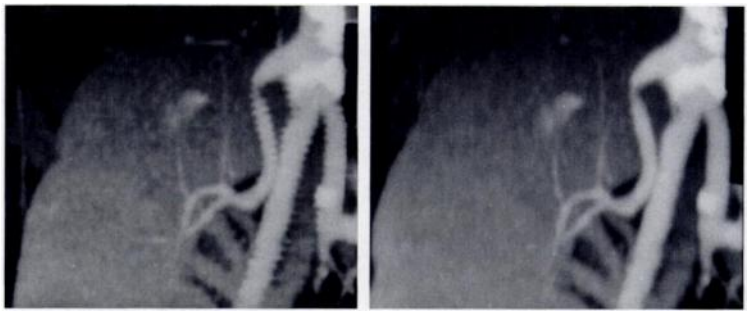

a. b.

Figure 25. **(a)** MIP image formatted with 180° interpolation demonstrates pulsation artifacts in a patient with a kidney transplant and renal artery stenosis. **(b)** MIP image obtained after spiral CT raw data are reconstructed with 360° interpolation shows reduction of the artifact.

• Respiratory Motion Artifacts

Large vessels that run perpendicular to the scan plane, such as the thoracic or abdominal aorta, are hardly affected by artifacts caused by respiratory motion. However, small vessels that run obliquely through the scan plane, such as almost all smaller abdominal side branches, are very vulnerable to such breathing effects. To reduce the frequency of respiratory motion artifacts, it is mandatory to instruct patients carefully in proper breath holding.

Artifacts caused by insufficient breath holding may be hard to distinguish from real disease. Breathing-related vessel movements may simulate stenoses or aneurysms (Fig 26) or may obscure abnormalities. Careful observation of organ and skin contours and comparison of the vessel of interest with other vessels at the same scan level or on the contralateral side are helpful for detecting motion artifacts. Use of caudocranial views may further help reduce the possibility that such artifacts are mistaken for disease.

• Other Pitfalls

Patient motion often leads to steplike artifacts and major discontinuities in vascular structures. Fortunately, these artifacts are rare and easy to distinguish from vascular abnormalities.

Because information about CT numbers is retained, MIP is very sensitive to inhomogeneous intravascular contrast: Small vessels that are not yet fully enhanced may not be displayed. In general, however, contrast inhomogeneities are rarely mistaken for vascular disease.

■ SUMMARY AND CONCLUSIONS

MIP is used to create angiography-like images from spiral CT data sets and is therefore an important and popular display tool in CT angiography (3–5,16–18). MIP images are not threshold dependent and preserve information about differences in attenuation. Thus, they often yield acceptable results even in cases in which SSD images fail because of threshold problems (4,5). MIP images are particularly useful for depicting small vessels. If anatomic structures are superimposed over the vessel of interest (eg, the renal veins may be superimposed over the renal artery), the MIP technique is often able to provide images of diagnostic quality as long as the contrast of the vessel of interest is sufficiently high compared with the surrounding structures. Preservation of attenuation information allows for discrimination between calcified and noncalcified vessel portions (3). MIP images therefore are an ideal display medium to demonstrate preoperatively calcified vessel walls for planning the site of anastomosis for bypass surgery (16).

On the other hand, MIP is a rather simple projection technique that does not allow for differentiation between foreground and background. A particular pixel in an MIP image may arise from any voxel along the projection ray. If two vessels are superimposed, the vessel with the higher CT number is displayed. In most CT angiographic applications, however, all major arteries at the same scan level have an identical CT number. Thus, the MIP image will show only the silhouette of the combined vascular structures. MIP images are therefore best suited to display relatively simple anatomic situations in which superimposition of structures does not occur, such as the abdominal aorta or pel-

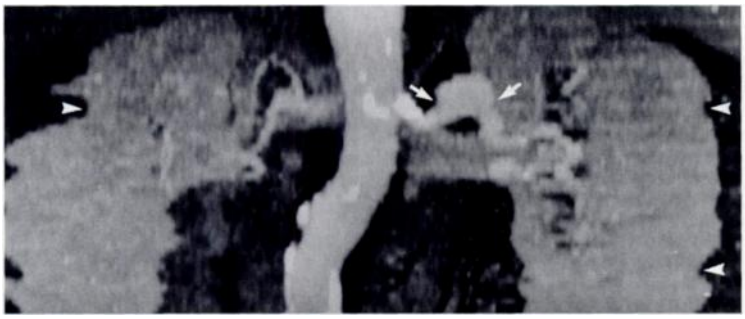

Figure 26. MIP image shows respiratory motion artifacts that simulate a renal artery aneurysm (arrows). Note the deformations of the contours of the kidneys, which indicate continued breathing artifacts (arrowheads).

vic arteries (4,16,19). MIP images do not allow visualization of vessel portions that are obscured by calcified plaque (20). Intraluminal abnormalities will not be demonstrated if contrasted portions of the vessel lumen are superimposed. Thus, evaluation of thrombi, emboli, or dissections is difficult with MIP (Figs 5, 6).

Even if overlapping image reconstruction is performed, the effective section thickness in CT angiography limits the spatial resolution along the patient axis (z axis). Thus, spatial resolution in anteroposterior MIP images (or any other projection angle perpendicular to the z axis) is limited by the effective section thickness. The attenuation profile (ie, the vessel profile) and the contrast of small vascular structures are strongly influenced by the vessel course relative to the scan plane: Because of partial volume averaging effects, the contrast of vessels that run parallel to the scan plane is reduced and the vessel profile is widened (Fig 12), whereas the contrast and attenuation profile of vessels that run perpendicular to the scan plane are not influenced.

The anatomic background plays an important role in MIP images because background attenuation varies depending on the size of the VOI to be displayed. The higher the background attenuation, the smaller the contrast of a vascular structure in the resulting MIP image (Fig 7). In addition, higher background attenuation leads to a decrease in vessel diameter, may lead to an overestimation of stenoses, and may even simulate occlusions (Figs 8–10) (21). As a consequence, taking diameter measurements on MIP images should be avoided. Background attenuation increases with growing image noise but more so if contrast-enhanced structures are included in the VOI (Fig 7). Therefore, the VOI should be chosen as narrow as possible, and all objects with high CT numbers should be excluded to obtain optimal results (Figs 8, 22, 23).

Two main types of editing procedures for MIP can be distinguished: cutting functions, in which cut lines are used to separate the VOI from its surroundings, and region-growing procedures, in which connectivity algorithms are used to detect and exclude structures such as bones from the VOI. Cutting functions are easier to handle and allow for separation of areas in cases in which region-growing algorithms fail (ie, if bones and vessels touch or have similar CT numbers). A convenient way to simplify basic editing procedures includes slab editing, in which the cut line is not adjusted on each single image but in which the data volume is subdivided into appropriate stacks and the cut lines are adjusted only for each stack. In this way, the number of interactions can be dramatically reduced (eg, from some 120 images to about 10 slabs for CT angiography of the abdominal aorta).

In areas in which there is close proximity of bones and vessels, such as the skull base, 2D region-growing algorithms are more precise. When there is no direct contact between bones and arteries (eg, carotid arteries), 3D region-growing algorithms are more effective for removing skeletal structures. In the chest or abdomen, however, small lumbar or intercostal arteries usually provide a "connection" between bones and vessels; thus, 3D region-growing algorithms are effective only when used with other procedures. These might include erosion or dilation operators, which provide a separation between adherent bones and vessels. Here, however, no final conclusions about the practical usefulness are possible yet.

Segmentation requires between 5 minutes (renal arteries) and 45 minutes (chest), depending on the complexity of the anatomic region,

the computer power, and the available software. In general, there is a trend toward using semiautomated segmentation algorithms (22) because time requirements are still cumbersome. Time-consuming segmentation may be avoided in certain cases. For example, thin-slab MIP images in caudocranial projection (8) are useful for depicting the orifices of the abdominal aortic side branches (Figs 17, 18). Similarly, it may be helpful to use narrow VOIs for lateral MIP images of the carotid arteries or the abdominal arteries (celiac artery, superior mesenteric artery, inferior mesenteric artery) (Fig 19) or for anteroposterior MIP images of the pulmonary vessels. We propose use of advanced editing to exclude the aorta and to allow for selective display of branching vessels, such as the celiac artery and its branches (Fig 23). Also, by excluding contrast-enhancing renal cortex, small hilar renal branches may become visible on MIP images (Fig 22).

When compared with SSD, MIP is superior for demonstrating small vessels in cases in which threshold problems might occur (high image noise, low contrast). However, SSD is superior to MIP in cases in which the vessels are superimposed on each other or other structures; the more complex the anatomic situation, the better it is to use SSD (2,23). However, full diagnostic information is present only in the original cross-sectional data set that may be viewed as primary axial images or as multiplanar reconstructed images (5,9). Thus, MIP and SSD are *display* techniques that provide an overview of the anatomic situation. The cross-sectional data set should remain the basis for diagnosis. A rational use of MIP images for various diagnostic applications can be summarized as follows.

1. Head (circle of Willis). If only the circle of Willis (including only a small intracranial portion of the carotid arteries) is to be displayed, the skull base can be excluded from the data volume (24). In this case, editing of bones is simple and can be performed most easily by using 3D region-growing algorithms or, with slightly more effort, by using a slab editor. However, if more of the intraosseous portion of the carotid arteries are to be included, the MIP images require extensive and difficult data editing. Usually, the combination 2D region-growing and erosion and dilation algorithms is successful. A sufficiently low threshold must be chosen to avoid ghost artifacts of bone contours.

2. Carotid arteries. MIP can be used to display the carotid arteries. Attention must be paid to calcified plaques that obscure the vascular lumen on MIP images (20,25). The display modalities of choice are thin-slab MIP (parallel to the carotid bifurcation) and multiplanar reformation. The jugular veins enhance early after administration of contrast material; therefore, precise timing of the contrast material bolus (bolus triggering, test bolus) is needed to facilitate subsequent data editing. Editing can often be simplified by using 3D region-growing algorithms.

3. Thoracic aorta. MIP is not the method of choice for displaying aortic or pulmonary artery disease; SSD is the clearly superior mode for displaying the thoracic aorta. The work-up of pulmonary embolism and aortic dissection requires the use of axial images (26). MIP images are too unreliable for the detection of nonoccluding thrombi or intimal flaps. Data editing is time-consuming and cumbersome: for depicting the thoracic aorta, pulmonary vessels must be removed; for visualization of the pulmonary arteries, the chest wall, the heart, and, for lateral or oblique views, the contralateral hemithorax must be excluded.

4. Abdominal aorta. MIP is well suited for display of abdominal aortic aneurysms (4,16–19). Use of sliding thin-slab MIP images is the most efficient way to visualize the relationship between renal arteries and aortic aneurysms. However, one must choose a compromise between a sufficiently large scan range and high z-axis resolution. High vascular enhancement is necessary to detect accessory renal arteries. Semiautomatic editing procedures will be available soon (22).

5. Renal, hepatic, and mesenteric arteries. MIP is the display mode of choice for the renal (5,21) and mesenteric arteries. Hepatic arteries are best evaluated by using sliding thin-slab MIP. Precisely timed scans in an early arterial phase are required to avoid disturbing enhancement of veins (eg, renal, portal, or mesenteric veins). Because the accessory vessels are small, the highest possible z-axis resolution is necessary (12). The anteroposterior MIP images are susceptible to respiratory motion artifacts. Lateral MIP images are helpful for demonstrating the proximal portions of the celiac and mesenteric arteries. Full display of hepatic and mesenteric vessels requires data editing with removal of the aorta.

In summary, MIP images can be used most advantageously for depicting the abdomen. As with all 3D techniques, MIP reduces a 3D data volume to a two-dimensional image; thus, there is an inevitable loss of information that may

lead to misinterpretation. For this reason, MIP should not be used as the only evaluation technique. MIP images should always be interpreted together with the original transaxial data set.

Knowledge of display properties and artifacts is necessary for correct interpretation of MIP images. Knowledge of these properties helps one to create MIP images of optimal quality, to choose appropriate examination parameters, and to distinguish artifacts from disease.

■ REFERENCES

1. Kalender WA, Polacin A. Physical performance characteristics of spiral CT scanning. Med Phys 1991; 18:910-915.
2. Prokop M, Schaefer C, Doehring W, et al. Spiral CT for three-dimensional imaging of complex vascular anatomy (abstr). Radiology 1991; 181(P):293.
3. Napel S, Marks MP, Rubin GD, et al. CT angiography with spiral CT and maximum intensity projection. Radiology 1992; 185:607-610.
4. Rubin GD, Dake MD, Napel SA, et al. Three-dimensional spiral CT angiography of the abdomen: initial clinical experience. Radiology 1993; 186:147-152.
5. Galanski M, Prokop M, Chavan A, et al. Renal arterial stenoses: spiral CT angiography. Radiology 1993; 189:185-192.
6. Fishman EK, Magid D, Ney DR, et al. Three-dimensional imaging. Radiology 1991; 181:321-337.
7. Rubin GD, Beaulieu CF, Argiro V, et al. Perspective volume rendering of CT and MR images: applications for endoscopic imaging. Radiology 1996; 199:321-330.
8. Napel S, Rubin GD, Marks MP, et al. Sliding thin slab maximum intensity projection technique for improved visualization with CT scans and MR angiograms (abstr). Radiology 1993; 189(P):351.
9. Zeman RK, Berman PM, Silverman PM, et al. Diagnosis of aortic dissection: value of helical CT with multiplanar reformation and three-dimensional rendering. AJR 1995; 164: 1375-1380.
10. Brink JA, Heiken JP, Balfe DM, et al. Spiral CT: decreased spatial resolution in vivo due to broadening of section-sensitivity profile. Radiology 1992; 185:469-474.
11. Prokop M, Schaefer CM, Galanski M, et al. 3D imaging with spiral CT: experimental evaluation of object distortion (abstr). Radiology 1992; 185(P):127.
12. Brink JA, Lim JT, Wang G, et al. Technical optimization of spiral CT for depiction of renal artery stenosis: in vitro analysis. Radiology 1995; 194:157-163.
13. Polacin A, Kalender WA, Marchal G. Evaluation of section sensitivity profiles and image noise in spiral CT. Radiology 1992; 185:29-35.
14. Prokop M, Schaefer C, Kalender WA, Polacin A, Galanski M. Gefaessdarstellungen mit spiral-CT: der weg zur CT-angiographie. Radiologe 1993; 33:694-704.
15. Rubin GD. Three-dimensional helical CT angiography. RadioGraphics 1994; 14:905-912.
16. Costello P, Gaa J. Spiral CT angiography of abdominal aortic aneurysms. RadioGraphics 1995; 15:397-406.
17. Bluemke DA, Chambers TP. Spiral CT angiography: an alternative to conventional angiography. Radiology 1995; 195:317-319.
18. Zeman RK, Silverman PM, Vieco PT, Costello P. CT angiography. AJR 1995; 165:1079-1088.
19. Richter CS, Biamino G, Ragg C, Felix R. CT angiography of the pelvic arteries. Eur J Radiol 1994; 19:25-31.
20. Castillo M, Wilson JD. CT angiography of the common carotid artery bifurcation: comparison between two techniques and conventional angiography. Neuroradiology 1994; 36:602-604.
21. Rubin GD, Dake MD, Napel S, et al. Spiral CT of renal artery stenosis: comparison of three-dimensional rendering techniques. Radiology 1994; 190:181-189.
22. Fishman EK, Liang C, Kuszyk BS, et al. Automated bone removal algorithm for 3D vascular CT: technique and preliminary clinical results (abstr). Radiology 1995; 197(P):222.
23. Katz M, Konen E, Rozenman J, Szeinberg A, Itzchak Y. Spiral CT and 3D image reconstruction of vascular rings and associated tracheobronchial anomalies. J Comput Assist Tomogr 1995; 19:564-568.
24. Katz DA, Marks MP, Napel SA, Bracci PM, Roberts SL. Circle of Willis: evaluation with spiral CT angiography, MR angiography, and conventional angiography. Radiology 1995; 195:445-449.
25. Marks MP, Napel S, Jordan JE, Enzmann DR. Diagnosis of carotid artery disease: preliminary experience with maximum-intensity-projection spiral CT angiography. AJR 1993; 160:1267-1271.
26. Remy-Jardin M, Remy J, Wattinne L, Giraud F. Central pulmonary thromboembolism: diagnosis with spiral volumetric CT with the single-breath-hold technique—comparison with pulmonary angiography. Radiology 1992; 185:381-387.

This article meets the criteria for 1.0 credit hour in Category 1 of the AMA Physician's Recognition Award. To obtain credit, see the questionnaire on pp 473-478.